Graphical Abstract

Incorporating Convection into the Solution-Diffusion Framework Enhances Modeling Accuracy in Reverse Osmosis

Mingheng Li, Joseph Li

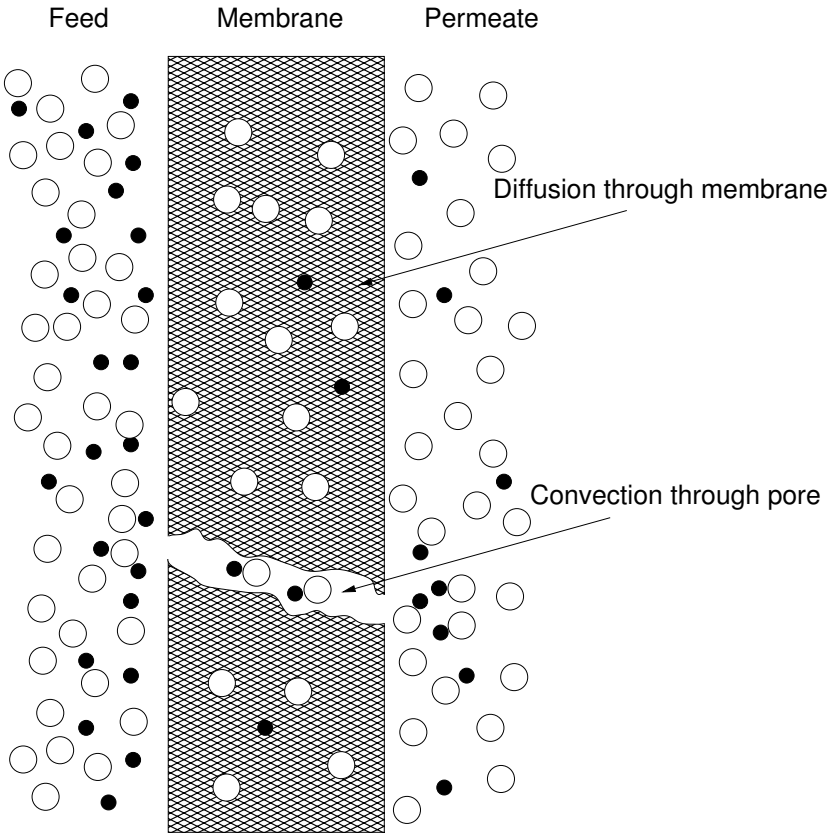

Highlights

Incorporating Convection into the Solution-Diffusion Framework Enhances Modeling Accuracy in Reverse Osmosis

Mingheng Li, Joseph Li

- Developed multiple linear correlation equations based on the solution-diffusion theory.
- Identified inconsistencies within the solution-diffusion model through extensive data analysis.
- Improved model accuracy by integrating convective transport across the membrane.

Incorporating Convection into the Solution-Diffusion Framework Enhances Modeling Accuracy in Reverse Osmosis

Mingheng Li[a,*], Joseph Li[b]

[a]*Department of Chemical and Materials Engineering, California State Polytechnic University, Pomona, CA 91768 USA*
[b]*Department of Chemical and Biomolecular Engineering, University of California, Berkeley, CA 94720 USA*

Abstract

Several linear correlation equations are derived from the classical solution-diffusion theory and applied to analyze over 100 experimental datasets collected under constant and sinusoidally varying feed flows and pressures. While the theory provides reasonable predictions for water flux, it fails to accurately model permeate concentration, particularly in cases of membrane degradation. Incorporating convective transport over a small portion of the membrane successfully captures the recovery rate and permeate quality across all scenarios studied ($R^2 \geq 0.99$). This enhanced model, with only three parameters, holds significant potential for advancing future membrane transport modeling efforts.

Keywords: reverse osmosis; solution-diffusion; transport modeling; data analysis; convection

1. Introduction

Transport modeling of water and salt is critical for the design and optimization of reverse osmosis (RO) desalination processes. The solution-diffusion model remains the most widely adopted framework for RO modeling [1]. According to this theory, the membrane is considered non-porous or characterized by extremely small pores, effectively preventing convective

*Corresponding author. Tel: 909-869-3668. E-mail: minghengli@cpp.edu

https://doi.org/10.1016/j.cherd.2025.01.012

transport of salts. Separation is achieved through the dissolution of water and salts into the membrane, followed by diffusion driven by concentration gradients. The solution-diffusion model relies on two key parameters: water permeability and salt permeability. When combined with pressure drop and mass transfer correlations, it provides reasonably accurate predictions of RO performance [2].

Recent advancements in transport modeling have introduced the solution-friction model [3], which is based on a pore-flow mechanism. This model accounts for interactions between water molecules and salt ions, as well as the force balances acting on the species moving through the membrane. For neutral solutes, and in the absence of friction between solutes and the membrane matrix, the solution-friction model simplifies to the Spiegler-Kedem-Katchalsky model [4], which was derived from irreversible thermodynamics. While the solution-friction model may offer a deeper mechanistic insight into water and salt transport in membranes [3], it introduces additional parameters, thereby increasing numerical complexity during the implementation of large-scale RO design and optimization.

This study aims to develop a simple yet accurate model for water and salt transport. The data used for model development were sourced from the literature, involving tests on a single FilmTec™ SW30-2540 spiral-wound element under constant and periodically varying flows and pressures [5]. A summary of these data is presented in Table 1, which is accessible via Mendeley Data (DOI: 10.17632/hws49dsfvc.1). Experiments categorized under the "sst" case in Table 1 were performed with a new membrane element, whereas data under the "ssr" case were collected after membrane degradation. In the degraded state, the membrane exhibited a slight increase in water permeability but a substantial surge in salt passage [5].

An analysis of these data using the classical solution-diffusion theory revealed intrinsic inconsistencies, which could potentially be resolved by incorporating an additional salt transport mechanism into the model.

2. Methods and Results

2.1. Solution-diffusion model

Based on the traditional solution-diffusion theory, the water and salt transport equations are as follows:

$$J_w = L_p[(P_r - P_p) - (\pi_w - \pi_p)] \quad (1)$$

Table 1: Experimental data sets from literature [5].

Case	Description	Feed rate (l/min)	Pressure (bar)	Recovery
sst	35 data sets under steady state feed flow and pressure conditions	6-16	34-60	3-23%
sin	45 data sets under sinusoidally varying flows and pressures	8-12*	41-55*	7-14%
sss	12 data sets under steady state conditions after sinusoidal experiments	10-12	35-60	3-14%
ssr	12 data sets under steady state conditions after rectified sinusoidal experiments that led to membrane degradation	10-12	34-60	3-16%

* These are cycle-average values reported by the authors. The instantaneous flow and pressure are estimated to be 5-15 l/min and 25-70 bar, respectively.

and

$$J_s = B_s(C_w - C_p) \tag{2}$$

where J_w and J_s represent water and salt fluxes, respectively. L_p and B_s are the water and salt permeability coefficients, respectively. P_r and P_p are the hydraulic pressures in the retentate and permeate channels, respectively. π_w and π_p are the osmotic pressures at the membrane wall and in the permeate, respectively, while C_w and C_p are the salt concentration at the membrane wall and in the permeate, respectively. When the salt concentration is low, it exhibits a linear relationship with osmotic pressure, i.e., $\pi = f_{os}C$, where f_{os} is a coefficient.

The average water and salt fluxes can be calculated by integrating Equations (1) and (2) over the spatial domain and dividing the results by the membrane area:

$$\begin{aligned} \bar{J}_w &= L_p[(\overline{TMP} - (\bar{\pi}_w - \bar{\pi}_p)] \\ &= L_p[(\overline{TMP} - f_{os}(\bar{C}_w - \bar{C}_p)] \end{aligned} \tag{3}$$

and

$$\bar{J}_s = B_s(\bar{C}_w - \bar{C}_p) \tag{4}$$

where $\overline{TMP} = \bar{P}_r - \bar{P}_p$ is the spatial average (denoted by overbar) of the transmembrane pressure.

For a single RO element, where the recovery rate is typically low, it is reasonable to assume that the spatial variation in flux is minimal. Under these conditions, the spatial average of salt concentration in the bulk of the feed channel may be calculated as [6]:

$$\bar{C} = [-\ln(1-Y)/Y]C_0 \tag{5}$$

where subscript 0 denotes the inlet condition, and Y is the recovery rate. The term $-\ln(1-Y)/Y$ can be interpreted as the inverse of the logarithmic mean of 1 and $1-Y$. It is crucial to include this term for the analysis of a commercial RO element, as it differs significantly from a short membrane coupon test cell typically used in laboratory settings, where the recovery rate is likely much less than 1% [7].

Due to concentration polarization, the wall concentration (C_w) is higher than the bulk concentration (C). The concentration polarization factor (CPF) is given by $\exp(J_w/k_m)$, where k_m is the mass transfer coefficient. In the absence of a well-validated correlation for k_m, the following equation for CPF in a single RO element, as adopted by DuPont FilmTec for RO system design and analysis, may be used [8]:

$$CPF = \exp(0.7Y) \tag{6}$$

Given that the salt concentration in the permeate channel is much lower than in the feed channel under typical operating conditions, Equation (3) can be simplified as:

$$\bar{J}_w = L_p\{\overline{TMP} - \pi_0[-\ln(1-Y)/Y]CPF\} \tag{7}$$

where π_0 is the feed osmotic pressure. Rearranging Equation (7) yields:

$$\frac{\overline{TMP}}{\bar{J}_w} = \frac{[-\ln(1-Y)/Y]CPF}{\bar{J}_w}\pi_0 + \frac{1}{L_p} \tag{8}$$

The permeate salt concentration at the outlet of the RO channel (C_{po}) is

calculated as:

$$\begin{aligned} C_{po} &= \frac{\int_0^{A_m} J_s dA_m}{\int_0^{A_m} J_w dA_m} \\ &= \frac{\bar{J}_s}{\bar{J}_w} \end{aligned} \tag{9}$$

where A_m is the membrane area. Note that C_{po} is distinct from $C_p = J_s/J_w$, which is commonly used in the literature and may be applicable for a short membrane test cell.

Combining Equations (3), (4) and (9) gives:

$$\bar{J}_w = L_p[\overline{TMP} - \frac{f_{os}}{B_s} C_{po} \bar{J}_w] \tag{10}$$

or equivalently:

$$\frac{\overline{TMP}}{\bar{J}_w} = \frac{f_{os}}{B_s} C_{po} + \frac{1}{L_p} \tag{11}$$

By combining Equations (8) and (11) the parameter L_p can be eliminated:

$$\begin{aligned} C_{po} &= \frac{B_s}{f_{os}} \pi_0 \frac{[-\ln(1-Y)/Y]CPF}{\bar{J}_w} \\ &= B_s C_0 \frac{[-\ln(1-Y)/Y]CPF}{\bar{J}_w} \end{aligned} \tag{12}$$

Equation (12) can also be derived from Equations (4), (5) and (9) without assuming the linear relationship between salt concentration and osmotic pressure.

Equation (8) suggests that a plot of $\overline{TMP}/\bar{J}_w$ versus $[-\ln(1-Y)/Y]CPF/\bar{J}_w$ should yield a straight line. The slope and intercept of this line correspond to π_0 and $1/L_p$, respectively. Similarly, Equation (11) indicates that a plot of $\overline{TMP}/\bar{J}_w$ versus C_{po} should yield a straight line, where the slope and intercept are f_{os}/B_s and $1/L_p$, respectively. Furthermore, Equation (12) suggests that a plot of C_{po} versus $C_0[-\ln(1-Y)/Y]CPF/\bar{J}_w$ should yield a straight line passing through the origin, with the slope equal to B_s.

The correlation results for all data sets using Equation (8) are shown in Figure 1(a). The feed osmotic pressure π_0 is determined to be 25.2 bar for case "sst" and 25 bar for case "ssr", which are slightly lower than the value calculated based on the experimental conditions (35,000 ppm TDS in the feed and 27 ℃), yielding a value of 26 bar [9]. The water permeability coefficient (L_p) is 1.06 lmh/bar for case "sst" and higher in case "ssr" at 1.16 lmh/bar, as observed by the authors who conducted the experiments [5]. Notably, the straight line derived from case "sst" correlates the data in cases "sin" and "sss" very well, and it is parallel to the straight line derived from case "ssr".

The correlation results for all data sets using Equation (11) are shown in Figure 1(b). The data appear to be divided into two distinct groups. While linear correlations are observed, some discrepancies cannot be reconciled. First, the value of L_p for case "sst" is determined to be 1.51 lmh/bar, which differs by more than 40% from the value shown in Figure 1(a). Second, the case of "ssr" exhibits a negative intercept, leading to a negative, non-physical L_p. Finally, when L_p and f_{os}/B_s, based on Figure 1(b), are combined with Equations (4) and (9) to calculate C_{po}, under-predictions occur, as shown in Figure 2. The average error is -15%.

This discrepancy is also evident in the correlation results derived from Equation (12). As illustrated in Figure 1(c), the straight lines do not pass through the origin. In the case of "sst", based on a brand-new membrane [5], the slope and intercept are 0.057 lmh and 26 ppm, respectively. In the case of "ssr", the slope and intercept are 0.126 lmh and 226 ppm, respectively.

These intrinsic inconsistencies within the theoretical framework of the solution-diffusion theory suggest the presence of additional mechanisms for salt transport. For example, if a small portion of the membrane is defective, it may provide an alternative pathway for salt to pass through the membrane. In fact, commercial RO membranes often feature minor structural imperfections, such as microvoids, cracks, or pinholes, which can notably influence salt rejection [10]. Furthermore, chemical attacks, excessive pressures, and the deposition of foulants can worsen these existing defects. The concept of incorporating defects into the solution-diffusion model is not new; it was presented by Eriksson at FilmTec over three decades ago [10]. Similar approaches have also been intermittently applied to pressure assisted forward osmosis [11], pressure retarded osmosis [12], and RO [13]. However, it has never gained widespread attention.

It is important to note that extreme pressure fluctuations can potentially cause leakage at the glue seams holding the RO element together. While

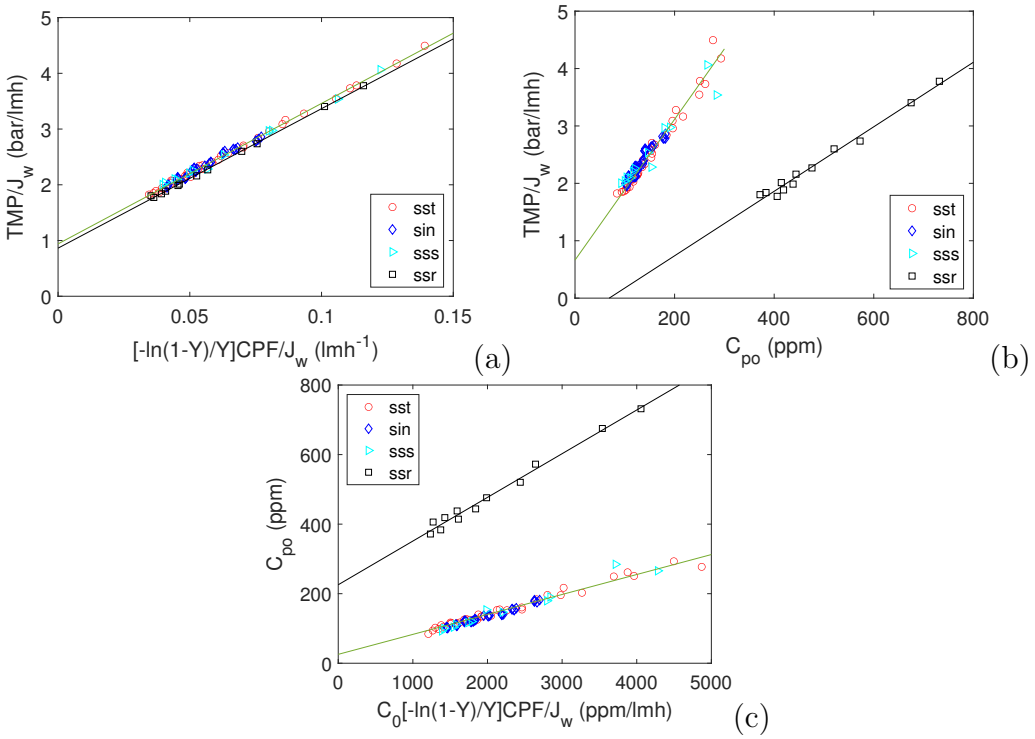

Figure 1: Correlation between (a) $\overline{TMP}/\bar{J}_w$ and $[-\ln(1-Y)/Y]CPF/\bar{J}_w$, (b) $\overline{TMP}/\bar{J}_w$ and C_{po}, and (c) C_{po} and $C_0[-\ln(1-Y)/Y]CPF/\bar{J}_w$. The two straight lines are based on cases "sst" and "ssr", respectively.

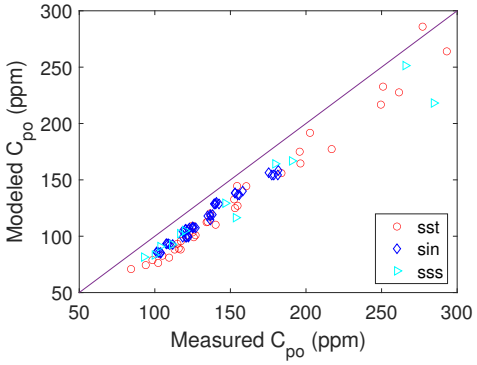

Figure 2: Under-predictions of permeate concentration by the solution-diffusion model.

this mechanism may help explain the increased water flux and reduced salt rejection observed in case "ssr", it does not appear to account for the under-predictions of permeate salinity in case "sst", where a new membrane element was used [5].

2.2. Solution-diffusion-with-defects model

It is assumed that the defects are uniformly distributed over the entire membrane area. The flow through the defective pores is proportional to the TMP. Additionally, salt transport through the defects is fully convective and is not subject to concentration polarization. The water and salt transport equations are as follows:

$$J_w = L_p[(P_r - P_p) - (\pi_w - \pi_p)] + \beta L_p[(P_r - P_p)] \tag{13}$$

and

$$J_s = B_s(C_w - C_p) + \beta L_p[(P_r - P_p)]C \tag{14}$$

where β ($\ll 1$) represents the membrane's defect ratio, and C is the salt concentration in the bulk of the feed channel.

Following the approach outlined in the previous section, the average flux and the concentration of the final permeate product can be calculated as:

$$\begin{aligned} \bar{J}_w &= L_p\{\overline{TMP} - \pi_0[\ln(1/(1-Y))/Y]CPF\} + \beta L_p\overline{TMP} \\ C_{po} &= \frac{(B_sCPF + \beta L_p\overline{TMP})C_0[\ln(1/(1-Y))/Y]}{\bar{J}_w} \end{aligned} \tag{15}$$

The parameters (L_p, B_s, β and π_0) are determined by minimizing the relative discrepancy between the measured and modeled flux and permeate concentration. Mathematically, this is formulated as:

$$\begin{aligned} \min_{L_p,B_s,\beta,\pi_0} J &= \sum_i \left(\frac{\bar{J}_{w_i}^{model}}{\bar{J}_{w_i}^{exp}} - 1\right)^2 + \left(\frac{C_{po_i}^{model}}{C_{po_i}^{exp}} - 1\right)^2 \\ s.t. & \\ & \text{Equation (15)} \end{aligned} \tag{16}$$

The results are $L_p = 1.06$ lmh/bar, $B_s = 0.044$ lmh, and $\beta = 0.05\%$ for case "sst" and $L_p = 1.15$ lmh/bar, $B_s = 0$, and $\beta = 0.49\%$ for case "ssr". In either case, $\pi_0 = 25.1$ bar. Notably, the hydraulic permeability coefficients

and the feed osmotic pressure are almost identical to those shown in Figure 1(a). The defect ratio is so small that it has virtually no impact on water permeation results, but it does affect salt passage. In this context, the classical solution-diffusion theory provides excellent results for water transport in high-salt-rejection membranes, even when these "defects" are completely ignored.

The B_s for case "sst" appears to be close to the value for SW30 membranes reported in literature [13]. However, for case "ssr", it remains unclear whether the deviation is due to convective transport through defects overshadowing diffusion or the limited number of data points (i.e., 12). Interestingly, by setting a minimum value for the parameter B_s in case "ssr", results can still be obtained that, although suboptimal, remain reasonably accurate. A sensitivity analysis reveals that as B_s increases from 0 to 0.1 lmh, the value of β that best fits the data decreases from 0.49% to 0.29%, while L_p and π_0 remain nearly constant. The objective function J in Equation (16) increases monotonically from 0.018 to 0.095, signifying a gradual decrease in correlation. If β is constrained to zero, the model fails to establish a strong correlation with salt concentration, underscoring the critical role of convective transport. Further investigation, supported by additional data points, may be necessary to determine the optimal pairing of B_s and β. If B_s in case "ssr" is assumed to be no less than the value for the new membrane, the parameters are determined to be $B_s = 0.044$ lmh, $\beta = 0.4\%$, $L_p = 1.15$ lmh, and $\pi_0 = 25.1$ bar.

Based on the complete experimental dataset, the pressure drop in the feed channel (ΔP_L) is correlated as a function of the average flow rate in the feed channel:

$$\Delta P_L = 0.0277 \left[\frac{Q_f + Q_f(1-Y)}{2} \right]^{1.45} \tag{17}$$

where ΔP_L is measured in bar, and the feed rate (Q_f) is in L/min. Using the specified membrane parameters, along with the feed rate, feed pressure (P_f), and feed osmotic pressure as inputs, the enhanced model and the pressure drop equation are solved simultaneously to determine the recovery rate, average water flux, and permeate concentration. The procedure for solving the predictive model is as follows:

1. Given L_p, B_s, β, π_0, Q_f, P_f and A_m.
2. Assume a recovery Y.

3. Calculate pressure drop (Equation (17)), $\overline{TMP}$, and CPF (Equation (6)).
4. Calculate $\bar{J}_w$ and C_{po} from Equation (15).
5. Calculate recovery $Y = \bar{J}_w A_m / Q_f$.
6. Compare the calculated recovery with the assumed recovery. If the difference is within the specified threshold, report the results and exit. Otherwise, proceed to step 2.

The above procedure is implemented in MATLAB using the `fsolve` function. The modeling results and their corresponding measurements are shown in Figure 3. The model with parameters derived from case "sst" provides accurate predictions for cases "sst" as well as "sin" and "sss". This serves to cross-validate the model for the membrane before the occurrence of degradation. The correlation results, with $R^2 \geq 0.99$ for both the recovery rate and permeate quality across the entire dataset, demonstrate the excellent performance of the enhanced model.

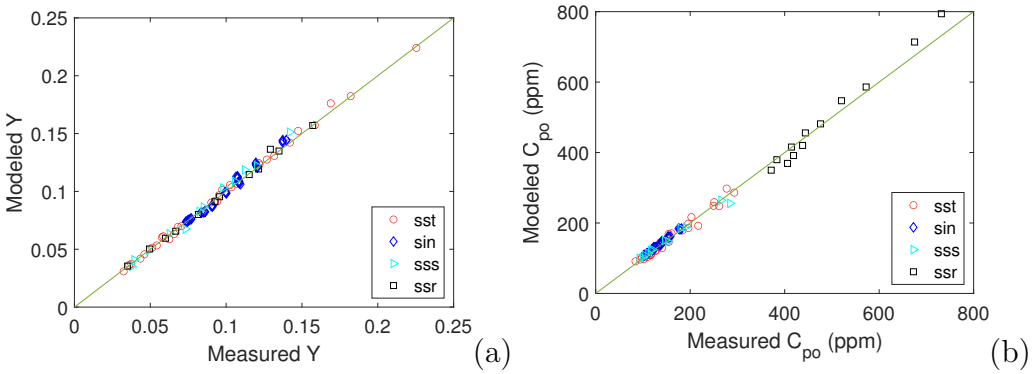

Figure 3: Comparison between solution-diffusion-with-defects model and experiment for (a) recovery ($R^2 \geq 0.99$) and (b) permeate concentration ($R^2 \geq 0.99$). The model is based on $L_p = 1.06$ lmh/bar, $B_s = 0.044$ lmh and $\beta = 0.05\%$ for cases "sst", "sin", and "sss" and $L_p = 1.15$ lmh/bar, $B_s = 0.044$ lmh and $\beta = 0.4\%$ for case "ssr". $\pi_0 = 25.1$ bar in all cases.

If the convective salt transport through the leak is assumed to be influenced by concentration polarization (or C in Equation (14) is replaced by C_w), the model yields results that are nearly identical to those shown in Figure 3, with only slight differences in B_s and β (For example, $B_s = 0.049$ lmh, $\beta = 0.04\%$ for case "sst").

It is important to note that the model presented in this study assumes a constant CPF and negligible variation in water flux, which are reasonable

simplifications for a single RO element. For a pressure vessel containing multiple elements arranged in series, the system can be analyzed sequentially by using the outlet conditions of one element as the inlet conditions for the next [8].

3. Conclusions

This work introduces several data correlation methods for one RO element. For the classical solution-diffusion model, plotting $\overline{TMP}/\bar{J}_w$ against $[-\ln(1-Y)/Y]CPF/\bar{J}_w$ should result in a straight line, with the slope and intercept corresponding to π_0 and $1/L_p$, respectively. Similarly, plotting C_{po} versus $C_0[-\ln(1-Y)/Y]CPF/\bar{J}_w$ is expected to yield a straight line passing through the origin, with the slope representing B_s.

An analysis of 104 datasets from the literature revealed intrinsic discrepancies that cannot be reconciled within the solution-diffusion model framework. Introducing an additional salt transport mechanism provides a plausible explanation for the under-predicted salt passage.

By incorporating a small membrane defect ratio into the solution-diffusion model, the enhanced approach effectively correlates water recovery and permeate quality across all cases of interest, including both intact membranes and those that have undergone degradation. This improved model relies on just three parameters–membrane permeability, salt permeability, and membrane defect ratio–making it straightforward to apply for RO modeling and optimization. However, this does not imply that the model is applicable to all cases of membrane degradation, as different types of degradation may exhibit distinct characteristics.

Acknowledgements

The authors would like to acknowledge financial support from the National Science Foundation (CBET-2140946). Any opinions, findings, and conclusions or recommendations expressed in this material are those of the authors and do not necessarily reflect the views of the National Science Foundation.

References

[1] J. G. Wijmans, R. W. Baker, The solution-diffusion model: a review, J. Membr. Sci. 107 (1995) 1–21.

[2] M. Li, T. Bui, S. Chao, Three-dimensional CFD analysis of hydrodynamics and concentration polarization in an industrial RO feed channel, Desalination 397 (2016) 194–204.

[3] L. Wang, J. He, M. Heiranian, H. Fan, L. Song, Y. Li, M. Elimelech, Water transport in reverse osmosis membranes is governed by pore flow, not a solution-diffusion mechanism, Sci. Adv. 9 (15) (2023) eadf8488.

[4] K. S. Spiegler, O. Kedem, Thermodynamics of hyperfiltration (reverse osmosis): criteria for efficient membranes, Desalination 1 (1966) 311–326.

[5] T. K. Das, M. Folley, P. Lamont-Kane, C. Frost, Performance of a SWRO membrane under variable flow conditions arising from wave powered desalination, Desalination 571 (2024) 117069.

[6] M. Li, Predictive modeling of a commercial spiral wound seawater reverse osmosis module, Chem. Eng. Res. Des. 148 (2019) 440–450.

[7] Aquaporin, `https://aquaporin.com/wp-content/uploads/2024/07/Aquaporin-Inside-Flat-Sheet-Membrane-Manual-Coupon-Performance-20240606.pdf`, online; accessed December 30, 2024 (2024).

[8] Dupont, FilmTec Reverse Osmosis Membranes Technical Manual, `https://www.dupont.com/content/dam/dupont/amer/us/en/water-solutions/public/documents/en/45-D01504-en.pdf`, Online; accessed April 25, 2020 (2020).

[9] K. G. Nayar, M. H. Sharqawy, L. D. Banchik, J. H. Lienhard V, Thermophysical properties of seawater: A review and new correlations that include pressure dependence, Desalination 390 (2016) 1–24.

[10] P. Eriksson, Water and salt transport through two types of polyamide composite membranes, J. Membr. Sci. 36 (1988) 297–313.

[11] J. Duan, E. Litwiller, I. Pinnau, Solution-diffusion with defects model for pressure-assisted forward osmosis, J. Membr. Sci. 470 (2014) 323–333.

[12] Z. M. Binger, G. O'Toole, A. Achilli, Evidence of solution-diffusion-with-defects in an engineering-scale pressure retarded osmosis system, J. Membr. Sci. 625 (2021) 119135.

[13] B. Blankert, K. T. Huisman, F. D. Martinez, J. S. Vrouwenvelder, C. Picioreanu, Are commercial polyamide seawater and brackish water membranes effectively charged?, J. Membr. Sci. Lett. 2 (2022) 100032.